

# Electromyography (EMG) Signal Contributions in Speed and Slope Estimation Using Robotic Exoskeletons

Inseung Kang<sup>1</sup>, *Student Member, IEEE*, Pratik Kunapuli<sup>2</sup>, Hsiang Hsu<sup>1</sup>, and Aaron J. Young<sup>1</sup>

**Abstract**—Robotic exoskeletons have the capability to improve community ambulation in aging individuals. These exoskeleton controllers utilize different environmental information such as walking speeds and slope inclines to provide corresponding assistance. Several numerical approaches for estimating this environmental information have been implemented; however, they tend to be limited during dynamic changes. A possible solution is a machine learning model utilizing the user's electromyography (EMG) signals along with mechanical sensor data. We developed a neural network-based walking speed and slope estimator for a powered hip exoskeleton and explored the EMG signal contributions in both static and dynamic settings while wearing the device. We also analyzed the performance of different EMG electrode placements. The resulting machine learning model achieved error rates below 0.08 m/s RMSE and 1.3° RMSE. Our study findings from four able-bodied and two elderly subjects indicate that EMG can improve the performance by reducing the error rate by 14.8% compared to the model using only mechanical sensors. Additionally, results show that using EMG electrode configuration within the exoskeleton interface region is sufficient for the EMG model performance.

**Index Terms**—Exoskeleton, Powered Orthosis, Electromyography (EMG), Machine Learning, Slope and Speed Estimation

## I. INTRODUCTION

The desire for the aging population to maintain an independent lifestyle is often impeded by limited community ambulation capability due to changes in their muscle tendon structures in the lower limb joints [1]. This reduced mobility leads to an inactive lifestyle and therefore decreases their overall quality of life. One possible solution to this problem is to utilize exoskeleton technology to provide assistance at the lower limb joints and enhance human movements. Different device and control strategies have been introduced from many research and industry groups to assist humans during locomotion [2]. For example, recent literature studies indicate that simple but effective assistance for the user (i.e. targeting a single joint) can increase overall exoskeleton performance as shown by the reduced metabolic cost during walking [3-5]. Our previous studies showed that this effective assistance relates to different control parameters for the exoskeleton, such as timing and magnitude, and that assistance levels can be optimized to maximize the human

exoskeleton performance [6, 7]. These control parameters are closely related with the user's state during locomotion such as walking speeds and slope levels. Having an accurate measurement of these state variables can aid the exoskeleton controller to shape the assistance profile correctly, thereby accommodating the environment and the user intent to maintain the overall exoskeleton performance.

Several estimation methods have been introduced to estimate both walking speeds and slopes [8, 9]. Most of them utilize a mechanical sensor such as an inertial measurement unit (IMU) and numerically compute the value, e.g. integrating a linear acceleration during certain phases of the gait cycle. However, this approach does not yield robust results to real-time implementation due to slow update rate and inaccurate estimation (i.e. sensor signal drifting over time). One possible solution is to implement a machine learning-based estimation strategy for its robustness in regressive tasks and real-time implementation capability. While utilizing different mechanical sensors from the exoskeleton may result in decent model accuracy, it may not comprehend the dynamic situations such as acceleration and decelerations with a high versatility. Moreover, for elderly subjects who may have different gait patterns on a stride-by-stride basis (mainly due to maintaining balance), mechanical sensor data may be insufficient for the model to robustly estimate these user states. One possible strategy to compensate for these limitations is to integrate a sensor fusion technique by utilizing human biological signals to enrich the user's state information for the machine learning model to learn [10].

Electromyography (EMG) has been studied heavily in the wearable robotics field for its advantage in providing valuable information about the user for exoskeleton control [11]. While some groups have utilized EMG as a control input to directly assist the user (i.e. proportional myoelectric controller) [12], others have employed EMG as a high-level control input to understand the user's intent, which have shown positive results [13, 14]. This idea of user intent can be expanded to speed and slope estimation especially in dynamic settings, where EMG may provide added information unique from the mechanical sensor data. While previous user intent recognition studies have shown the benefits of fusing mechanical sensors with EMG, to our knowledge, there has not been a study that explores the EMG contributions in estimating walking speeds and slopes for exoskeletons. Moreover, which muscles are optimal to use for improving user intent estimation with a hip exoskeleton has not been studied. Lastly, while several groups have investigated different strategies to estimate user state, these results were

\*This work was supported in part by the Georgia Tech Research Institute (GTRI) IRAD funding and the NSF NRI Award #1830215.

<sup>1</sup>I. Kang, H. Hsu, and A. Young are with the School of Mechanical Engineering, Georgia Institute of Technology, Atlanta, GA 30332 USA [ikang7@gatech.edu](mailto:ikang7@gatech.edu)

<sup>2</sup>P. Kunapuli is with the School of Electrical and Computer Engineering, Georgia Institute of Technology, Atlanta, GA 30332 USA

often focused on able-bodied subjects. It is critical to evaluate the translatability of this technology to mobility challenged elderly populations to verify the feasibility of these machine learning approaches.

In this study, we investigated the machine learning model performance in estimating the user's walking speed and slope while wearing a powered hip exoskeleton. The model utilized different combinations of mechanical and EMG data to observe if including the EMG signal provided additional value. Specifically, we focused on exploring how EMG can help overall performance when speeds and slopes are changed dynamically. Lastly, we looked into EMG contributions in machine learning models for elderly subjects who may have variable gait patterns. Our hypothesis is that EMG information can improve the overall machine learning model performance in estimating walking speed and slope, specifically when there is a high variation in user's gait dynamics. Our findings will provide valuable information for the exoskeleton designers to select optimal sensors to estimate the user's walking speed and slope, which can be used for improving adaptive control of an exoskeleton.

## II. POWERED HIP EXOSKELETON DESIGN

### A. Mechatronic Design

We developed an updated version of our previously designed powered hip exoskeleton (Fig. 1) [15]. Similar to the prior design, the exoskeleton employed a ball screw driven series elastic actuator (SEA) to drive the hip joint. The SEA torque measurement using fiberglass spring deflection allows operations of the device with a closed loop torque control. The main focus of the design changes were associated with modifying the overall structure of the frame (i.e. user interface) as well as interchanging the SEA components and orientation to maximize the exoskeleton performance.

The modified SEA units were oriented vertically to reduce the overall form factor of the actuator. The weight of each actuator was reduced from 1.5 kg to 0.9 kg with the modified design. Different from our previous design, new actuators were enclosed with a protective carbon fiber plate housing. These plates are supported with 3D printed structures that also provide a mechanical hard stop at the output joint. One of the main advantages in doing this is to leverage the transmission orientation to achieve desired SEA torque and velocity for different applications. Due to the nature of the ball screw driven actuator using the series spring as a lever arm, the gear ratio varies depending on the hip joint orientation. While our previous design achieved desired torque and velocity specification, it was achieved at an undesired location (i.e. at hip flexion of  $50^\circ$ ). To maximize the device performance, vertical orientation ensured the SEA would provide full assistance capability during walking. With this modification, the overall gear ratio of the system was reduced (by approximately half compared to our previous design) to 100:1. Our updated SEA achieved a peak torque of 30 Nm, continuous torque of 15 Nm and angular velocity of  $300^\circ/\text{sec}$ .

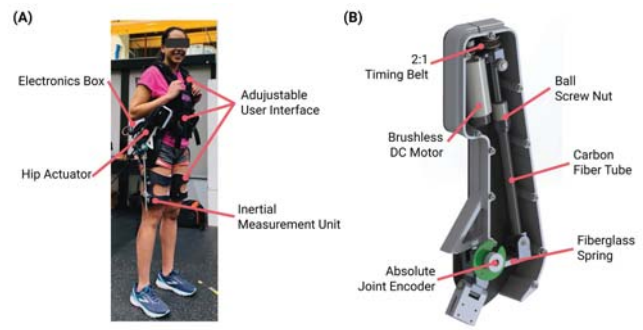


Fig. 1. Powered hip exoskeleton design. (A) The exoskeleton has the actuator attached bilaterally at each waist plate and the electronics box at the back plate. The user interface can be adjusted to accommodate different body sizes. (B) The series elastic actuator is oriented vertically with carbon fiber plate housing.

Our previous device used the commercially available orthotic interface to fit the exoskeleton to the user. This approach had major limitations in being inefficient in translating the hip joint assistance as well as causing discomfort to the user when used for long periods of time. This was mainly due to not fully accounting for different body shapes when interfacing the exoskeleton to the user [16]. Our new custom-made exoskeleton interface (Fillauer Companies) considered these factors and utilized conforming body plates to secure the user from four directions. Each interface has its own adjustable straps to ensure a secure fitting while the back and side plates are attached directly to the main C shaped frame. Our previous thigh cuff design was only capable of changing the cuff in discrete locations; the updated design can change the cuff locations continuously using a clamping mechanism. These interface modification vastly reduced the overall exoskeleton don/doff time from approximately 10 minutes to less than a minute.

### B. Control Layer Architecture

The exoskeleton control layers are broken down into three layers: high-, mid-, and low-level. The high-level control layer intakes different sensor data from the device (joint encoder, IMUs, and FSR at the heel) and estimates the user state in real-time such as the user gait phase, walking speed, and walking slope. Different estimators can be implemented in this layer (i.e. machine learning model) in parallel architecture and be computed simultaneously within the myRIO. Within the mid-level layer, the estimated user state variables from the high-level layer are used as a control parameter to compute the desired torque command to the user where the assistance controller can be of any form such as impedance controller [17] or biological torque controller [18]. During the time when the device is not providing assistance to the user, the device is set to zero impedance mode, where the commanded torque is 0 Nm to cancel out any residual interaction torque generated from the actuator transmission system. With the better device performance from the modified SEA design, the residual interaction torque in zero impedance mode was reduced from an average of 0.94 Nm

to 0.25 Nm during walking. After the torque command is set from the mid-level layer, the desired torque is commanded to the low-level layer where the closed loop torque control is performed with the SEA to ensure the desired torque is tracked in real-time. Since we were specifically interested in estimating the users walking speed and slope, the proposed study exclusively focused on the high-level layer.

### III. METHODS

#### A. Human Subject Experiment

The study was approved by the Georgia Institute of Technology Institutional Review Board, and informed written consent was obtained for all subjects. Four able-bodied subjects (three males and one female) with an average age of  $23.5 \pm 3.3$  years, height of  $1.79 \pm 0.08$  m, and body mass of  $73.3 \pm 4.6$  kg and two elderly subjects (both females) with an average age of 72.5 years, height of 1.67 m, and body mass of 73.5 kg participated in data collection. The elderly subjects were community ambulatory but walked with a reduced preferred walking speed of approximately 60%. All subjects were asked to walk on a treadmill (Bertec Corporation) while wearing the powered hip exoskeleton (Fig. 2A). The exoskeleton controller was set to zero impedance mode for all conditions. During walking, hip joint encoder, trunk IMU (Micro USB, Yost Lab), and thigh IMU data were collected

(6 DOF IMU streams accelerometer and gyroscope data). A total of 8 channel electrodes (Biometrics Ltd) were used for collecting EMG data: 1. proximal rectus femoris (PRF), 2. gluteus medius (GM), 3. rectus femoris (RF), 4. biceps femoris (BF), 5. vastus medialis (VM), 6. vastus lateralis (VL), 7. adductor magnus (AM), and 8. distal biceps femoris (DBF). Channels 3-8 EMG electrodes were located inside the exoskeleton thigh cuff region, while channels 1 and 2 EMG electrodes were placed outside the thigh cuff region at the proximal hip musculature.

The experiment had two parts: static and dynamic trials. During static trials, the able-bodied subjects walked on a level ground with speed ranging from 0.8 m/s to 1.2 m/s in 0.1 m/s increments. After, the subjects walked at incline with slope ranging from  $2^\circ$  to  $10^\circ$  in  $2^\circ$  increments and decline with slope ranging from  $-2^\circ$  to  $-10^\circ$  in  $2^\circ$  increments both at walking speeds of 0.8 m/s. For each of the speed and slope trials, subjects walked for one minute. For elderly subjects, the same protocol was followed except treadmill speeds and slope angles were set differently. This was done to accommodate the elder subjects' lower preferred walking speed and ambulation capabilities in different slopes. The treadmill speed range was set from 0.3 m/s to 0.7 m/s with 0.1 m/s increments and slope range was set from  $1^\circ$  to  $7^\circ$  with  $2^\circ$  increments with walking speed of 0.3 m/s.

During dynamic trials, the able-bodied subjects walked on a treadmill while the speed and slope (both incline and decline) were modulated by a predefined trajectory generated from the control desk (MATLAB, MathWorks). The speed profile contained both steady state section ranging from 0.8 m/s to 1.2 m/s as well as dynamic section where the treadmill accel/decelerates for 2 minutes (Fig. 2B). Similar profiles were generated for both incline and decline dynamic trials where the slope angles ranged from  $2^\circ$  to  $10^\circ$  both uphill and downhill walking at 0.8 m/s for 3 minutes. Similar to the static trial, elder subjects followed the same protocol except for the walking speeds and slope angles. For elder subjects, dynamic speed profile ranged from 0.3 m/s to 0.7 m/s for 2 minutes and slope profile ranged from  $1^\circ$  to  $7^\circ$  both uphill and downhill walking at 0.3 m/s for 3 minutes.

#### B. Data Analysis and Machine Learning Model

After the data collection, all EMG data (both able-bodied and elderly subjects) were processed with a bandpass filter (8th order Butterworth, 20 Hz  $\sim$  400 Hz) to remove any motion artifacts. For each subject, three different neural network models were generated from speed and slope walking conditions using different underlying sets of sensors: mechanical sensor data only (MECH), mechanical sensor and EMG data from 4 of the channels within the thigh cuff regions along with the additional two additional proximal EMG data (channels 1-6) (EMG1), and mechanical sensor with EMG data all from the thigh cuff region (channels 3-8) (EMG2). Overall channel number was kept consistent between the two EMG configurations for fairness of model comparison. For slope walking estimation, separate incline and decline models were generated: while a unified slope estimation model is possible,

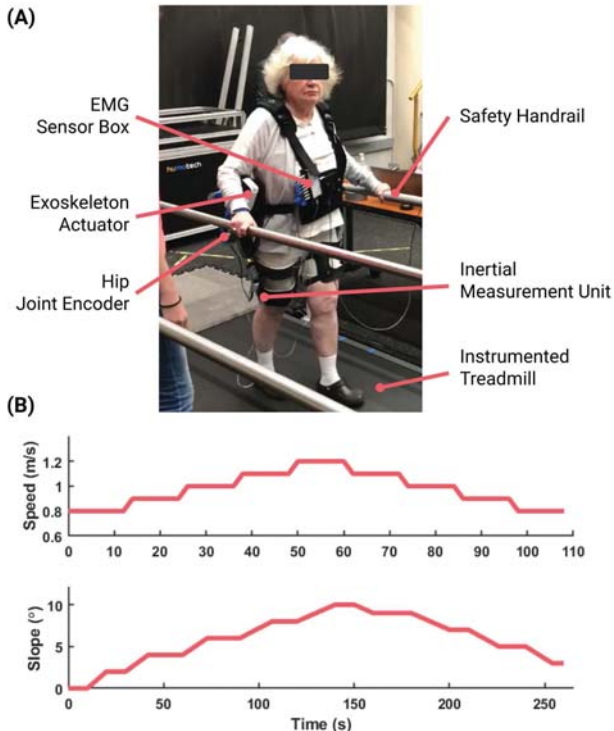


Fig. 2. Experimental setup for data collection. (A) The subject walked on the treadmill with varying speeds and slopes. The hip joint encoder, trunk IMU, thigh IMU, and 8 channel EMG data were collected during the experiment. (B) An example of able-bodied subject dynamic trial profile. The dynamic trials had predefined speed and slope ranges that changed while the user walked on the treadmill.

we were able to reduce the overall slope estimation error rate by nearly 40% by separating it into two. As literature studies have shown positive results in implementation of locomotion mode classification using machine learning [19, 20], we focused on increasing the overall accuracy of our models. For a real-time implementation, our models can be cascaded with a simple mode classifier.

We performed speed and slope estimation once per gait cycle at the time point corresponding to the peak hip extension angle (near toe off). This was a reliable gait point to detect based on the internal sensors available in the hip exoskeleton. We performed an analysis of the window size prior to this gait event to maximize walking speed and slope estimation accuracy. From this processed data, neural network models were trained for each sensor set combination following standard literature practices [21]. The finalized feature extraction were 4 features (minimum, maximum, mean, and standard deviation) for mechanical sensors and a single feature (mean absolute value) for EMG signals. The finalized feature extraction window size was a 500 ms. The neural network architecture and hyper-parameters were also swept with standard practices and the result was a single layer with 50 nodes, activated with a *tanh* function, and optimized by stochastic gradient descent. While we can improve the overall performance of the model by increasing the number of layers and nodes, we kept the overall structure relatively simple as this would be more realistic for future real-time implementation. Using corresponding data, neural network models were trained with aforementioned neural network architecture with Python using Keras [22]. The models were trained with data from static trials with 5-fold validation. We took the root mean squared (RMS) errors for each condition to evaluate the models' performance (static trial performance). For dynamic trials, all the data from the static trials were used to train the model and the entire dynamic trial was used to test the model. Similarly, we calculated the RMS error and compared the models' performances (dynamic trial performance). Lastly, we calculated the EMG signal contributions during trials by calculating the maximum mean absolute value for each walking condition. After, we observed the EMG activation levels as a function of walking speed or slope.

#### IV. RESULTS

##### A. Static Trial Performance

For able-bodied subjects (Fig. 3A), the average walking speed RMS errors across all static trial conditions were  $0.094 \pm 0.043$  m/s,  $0.077 \pm 0.012$  m/s, and  $0.076 \pm 0.017$  m/s for MECH, EMG1, and EMG2, respectively. For the incline, the average RMS errors were  $1.624 \pm 0.400^\circ$ ,  $1.288 \pm 0.176^\circ$  and  $1.431 \pm 0.307^\circ$  for MECH, EMG1, and EMG2, respectively. For the decline, the average RMS errors were  $1.620 \pm 0.633^\circ$ ,  $1.533 \pm 0.608^\circ$  and  $1.324 \pm 0.494^\circ$  for MECH, EMG1, and EMG2, respectively. For elderly subjects (Fig. 3B), the average walking speed RMS errors across all conditions were 0.061 m/s, 0.078 m/s, and 0.089 m/s for MECH, EMG1, and EMG2, respectively. For the incline,

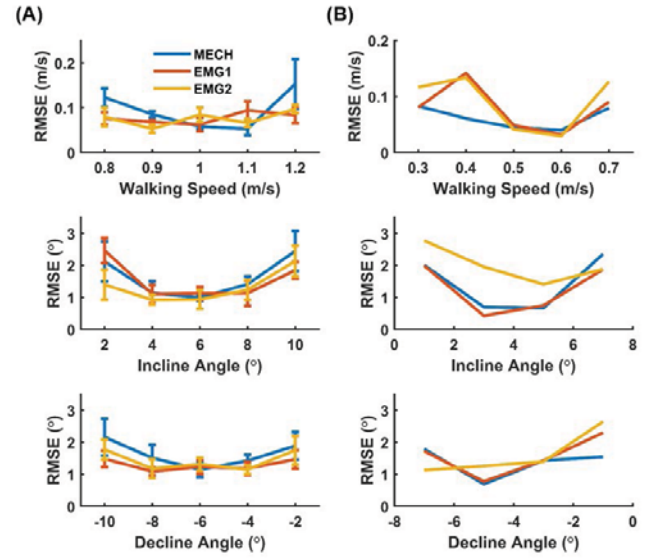


Fig. 3. Static trial model performance results for (A) able-bodied and (B) elderly subjects. Different colored lines indicate the models used for estimation. The RMS errors were averaged across all subjects. The error bars in the graph represents  $\pm 1$  SEM.

the average RMS errors were  $1.363^\circ$ ,  $1.556^\circ$  and  $1.604^\circ$  for MECH, EMG1, and EMG2, respectively. For the decline, the average RMS errors were  $1.431^\circ$ ,  $1.258^\circ$  and  $2.003^\circ$  for MECH, EMG1, and EMG2, respectively.

##### B. Dynamic Trial Performance

For able-bodied subjects (Fig. 4A) during dynamic trials, EMG1 and EMG2 reduced the average RMS walking speed error rates compared to the MECH by 15.2% and 23.3%, respectively. For the incline trials, EMG1 and EMG2 reduced the average RMS error rate compared to the MECH by 7.6% and 11.5%, respectively. For the decline trials, EMG1

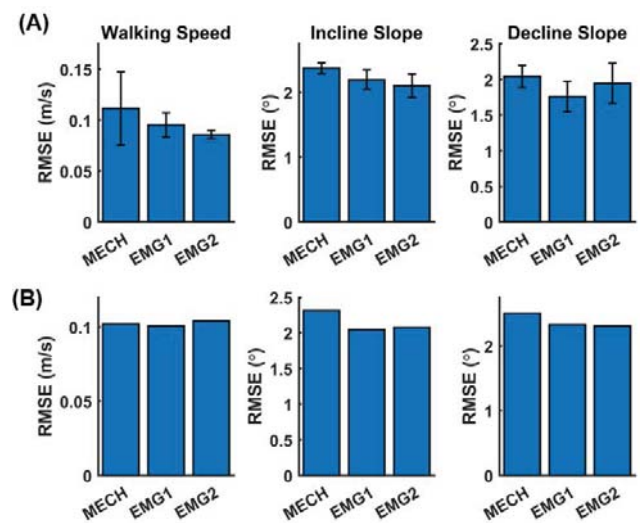


Fig. 4. Dynamic trial model performance results for (A) able-bodied and (B) elderly subjects. The RMS errors were averaged across all subjects. The error bars in the graph represents  $\pm 1$  SEM.

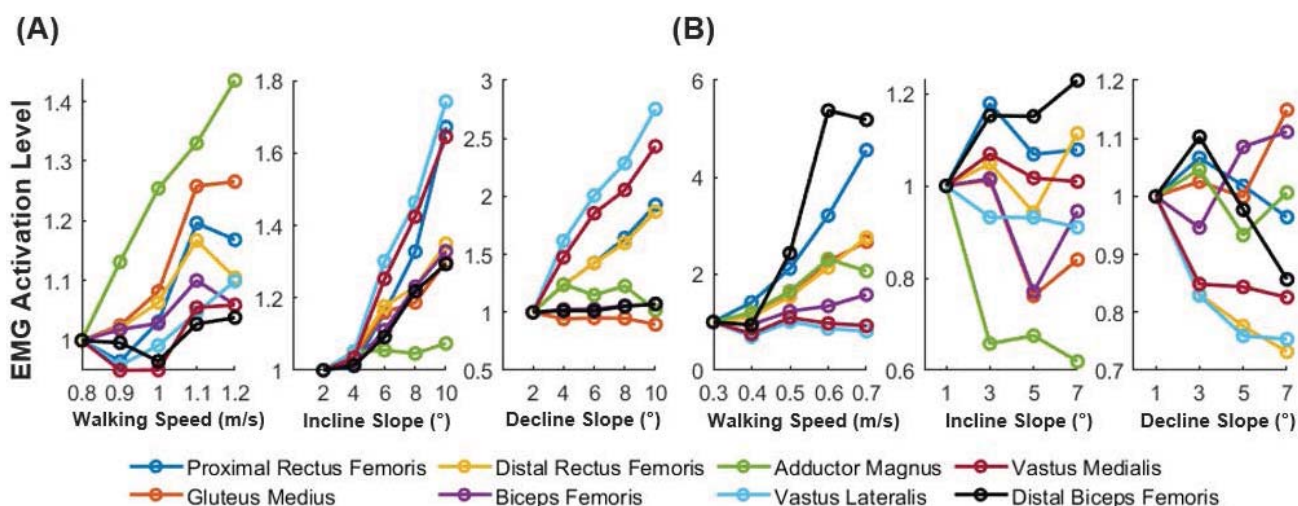


Fig. 5. Average EMG activation levels across different walking speeds and slopes for (A) able-bodied and (B) elderly subjects. The EMG signals are represented with the maximum mean absolute value for each walking conditions.

and EMG2 reduced the RMS error rate compared to the MECH by 14% and 4.8%, respectively. For elderly subjects (Fig. 4B) during dynamic trials, EMG1 reduced the average RMS walking speed error rate compared to the MECH by 1%. For the incline trials, EMG1 and EMG2 reduced the average RMS error rate compared to the MECH by 11.8% and 10.2%, respectively. For the decline trials, EMG1 and EMG2 reduced the average RMS error rate compared to the MECH by 7% and 7.9%, respectively.

### C. EMG Signal Analysis

For able-bodied subjects (Fig. 5A), the proximal hip muscle groups (AM, GM, and PRF) had greater rates of change in EMG activation with regards to different walking speeds. However, for different walking slopes, the distal knee extensor muscle groups (VL and VM) showed greater rates of change in EMG activation. On the other hand, elderly subjects (Fig. 5B) showed different EMG signal behavior: for walking speeds and incline slopes, both proximal and distal muscles had greater rates of change in EMG activation. For decline slopes, the distal knee extensor muscles (DRF, VL, and VM) showed greater rates of change in EMG activation. These results show that while able-bodied subjects increased their overall EMG activation with an increase in condition intensities, elderly subjects reduced EMG activation with an increase in slope angle.

## V. DISCUSSION

Overall, all three models were able to estimate the user's walking speeds and slopes. For able-bodied subjects, EMG models had better performance than the MECH by reducing the average estimation error rate by 13.5% and 14.8% across all trials for EMG1 and EMG2, respectively. While the able-bodied results indicate consistent performance of both EMG models in all cases, the results were not the same for the elderly subjects. EMG models only improved the estimation accuracy during dynamic trials compared to the

MECH with an average error rate reduction of 6.6% and 5.4% for EMG1 and EMG2, respectively. While the overall estimation accuracies were in similar orders of magnitude, the main reason for the elderly subjects' results may be due to stride-by-stride gait variations. As shown in Fig. 5, elderly subjects generally showed inconsistent EMG signal trends compared to that of the able-bodied subjects. This may have limited the machine learning model's ability to differentiate the walking conditions when EMG information was added. However, across all subjects, results were indicative of the EMG signals benefitting the machine learning model during dynamic trials.

One of the main reasons that the both EMG models outperformed the MECH model during dynamic trials was due to trial speed and slope trajectory having an accel/deceleration section. While mechanical sensors can provide sufficient information to solve a regression problem during steady state walking, they have a limitation of not being versatile in understanding the user's intention. EMG data plays a critical role in this sense where signal information can be used to predict the user's intention to either accelerate or decelerate. The capability of EMG information for user intent has already shown positive results in the literature for classifying locomotion mode transitions [13, 23]. Essentially, the role of EMG becomes greater in speed and slope estimation as regression is a continuous estimation of user intent when dynamically changing the underlying walking states. While our accel/deceleration profile had relatively mild changes in walking speeds and slopes, a more realistic setting (i.e. over ground walking including starting and stopping) will have greater variations in walking speeds and slopes where EMG contributions to maintain model accuracy may be greater.

Able-bodied subjects showed a consistent linear trend directionality in EMG activities with corresponding walking conditions. Generally, their proximal hip muscles were recruited more during walking speed trials while distal

knee muscles were recruited during slope walking. However, elderly subjects showed completely different muscle recruitment strategies. For example, during decline slope walking, elderly subjects reduced their distal knee extensor activation and relied more on the proximal hip extensors. One possible reason might be due to a subject's prioritization during walking. Able-bodied subjects tend to focus on power absorption to dissipate their COM energy in the downward direction during decline slope walking [24]. However, this may not be the case for elderly subjects, who instead prioritize maintaining stability during decline slope walking. Therefore, elderly subjects relied more on proximal muscles to maintain a desired trunk orientation.

Another key finding is that regardless of the model performances, EMG1 and EMG2 showed relatively similar results. This shows great promise in designing the exoskeleton that utilizing EMG electrodes placed within the thigh cuff region is adequate information to increase model accuracy. Additionally, this trend was the same across both subject groups, suggesting that a separate exoskeleton design for elders is unnecessary. While we cannot provide definite conclusion to our hypothesis due to low power with limited number of subjects, our preliminary results indicate that EMG data indeed contribute to increasing machine learning model accuracy in estimating a user's walking speeds and slopes during dynamic tasks. Lastly, another limitation of this study is that all the model analysis was done offline. Future study should include additional real-time implementation of the model with exoskeleton assistance to evaluate the estimator performance.

## VI. CONCLUSION

Our machine learning models were able to estimate the user's walking speeds and slopes accurately. The study results have shown that the EMG provides valuable information to increase the overall model performance in slope and speed estimation tasks. While able-bodied subjects improved the estimation accuracy using EMG in all trials, elderly subjects benefited from EMG only during dynamic tasks. Our findings indicate that, depending on the exoskeleton user, EMG contributes to improving model accuracy in estimating the user's walking speeds and slopes.

## ACKNOWLEDGMENT

The authors thank Dr. Geza Kogler for his insight with the exoskeleton interface design. We also thank Regu Nammalwar, Shahana Maji, Stella Thai, and Ana Groff for their help with the data collection. Finally, we thank David Taylor for recruiting elderly subjects for the experiment.

## REFERENCES

- [1] Narici, M.V., *et al.*, Effect of aging on human muscle architecture. *Journal of Applied Physiology*, 2003. 95(6): p. 2229-2234.
- [2] Young, A.J. and D.P. Ferris, State of the Art and Future Directions for Lower Limb Robotic Exoskeletons. *IEEE Transactions on Neural Systems and Rehabilitation Engineering*, 2017. 25(2): p. 171-182.
- [3] Seo, K., *et al.* Fully autonomous hip exoskeleton saves metabolic cost of walking. in *2016 IEEE International Conference on Robotics and Automation (ICRA)*. 2016.
- [4] Mooney, L.M., E.J. Rouse, and H.M. Herr, Autonomous exoskeleton reduces metabolic cost of human walking. *J Neuroeng Rehabil*, 2014. 11.
- [5] Ding, Y., *et al.*, Human-in-the-loop optimization of hip assistance with a soft exosuit during walking. *Science Robotics*, 2018. 3(15).
- [6] Kang, I., H. Hsu, and A. Young, The Effect of Hip Assistance Levels on Human Energetic Cost Using Robotic Hip Exoskeletons. *IEEE Robotics and Automation Letters*, 2019. 4(2): p. 430-437.
- [7] Malcolm, P., *et al.*, A simple exoskeleton that assists plantarflexion can reduce the metabolic cost of human walking. *PLoS one*, 2013. 8(2): p. e56137.
- [8] Li, Q., *et al.*, Walking speed estimation using a shank-mounted inertial measurement unit. *Journal of Biomechanics*, 2010. 43(8): p. 1640-1643.
- [9] Li, Q., *et al.* Walking speed and slope estimation using shank-mounted inertial measurement units. in *2009 IEEE International Conference on Rehabilitation Robotics*. 2009.
- [10] Young, A., T. Kuiken, and L. Hargrove, Analysis of using EMG and mechanical sensors to enhance intent recognition in powered lower limb prostheses. *Journal of neural engineering*, 2014. 11(5): p. 056021.
- [11] Kawamoto, H., *et al.* Power assist method for HAL-3 using EMG-based feedback controller. in *IEEE International Conference on Systems, Man and Cybernetics*. 2003. IEEE.
- [12] Koller, J., *et al.* Adaptive Gain for Proportional Myoelectric Control of a Robotic Ankle Exoskeleton During Human Walking. in *American Society for Biomechanics*. 2015. Columbus, OH.
- [13] Young, A. and L. Hargrove, A Classification Method for User-Independent Intent Recognition for Transfemoral Amputees Using Powered Lower Limb Prostheses. *IEEE Transactions on Neural Systems and Rehabilitation Engineering*, 2015.
- [14] Zhang, F. and H. Huang, Source Selection for Real-Time User Intent Recognition Toward Volitional Control of Artificial Legs. *IEEE Journal of Biomedical and Health Informatics*, 2013. 17(5): p. 907-914.
- [15] Kang, I., H. Hsu, and A.J. Young, Design and Validation of a Torque Controllable Hip Exoskeleton for Walking Assistance. in *ASME 2018 Dynamic Systems and Control Conference*. 2018. American Society of Mechanical Engineers.
- [16] Lee, S., *et al.*, Investigating the impact of the user interface for a powered hip orthosis on metabolic cost and user comfort: a preliminary study. *Journal of Prosthetic and Orthotics*, 2019 (*Under Review*).
- [17] Hogan, N., Impedance Control - an Approach to Manipulation .1. Theory. *Journal of Dynamic Systems Measurement and Control*, 1985. 107(1): p. 1-7.
- [18] Young, A.J., *et al.*, Influence of Power Delivery Timing on the Energetics and Biomechanics of Humans Wearing a Hip Exoskeleton. *Front Bioeng Biotechnol*, 2017. 5: p. 4.
- [19] Huang, H., T. Kuiken, and R. Lipschutz, A Strategy for Identifying Locomotion Modes using Surface Electromyography. *IEEE Trans Biomed Eng*, 2009. 56(1): p. 65-73.
- [20] Young, A., A. Simon, and L. Hargrove, A Training Method for Locomotion Mode Prediction Using Powered Lower Limb Prostheses. *IEEE Transactions on Neural Systems and Rehabilitation Engineering*, 2014. 22(3): p. 671-677.
- [21] Schmidhuber, J., Deep learning in neural networks: An overview. *Neural Networks*, 2015. 61: p. 85-117.
- [22] Chollet, F., Keras. 2015.
- [23] Huang, H., *et al.*, Continuous Locomotion-Mode Identification for Prosthetic Legs Based on Neuromuscular-Mechanical Fusion. *IEEE Transactions on Biomedical Engineering*, 2011. 58(10): p. 2867-2875.
- [24] Montgomery, J.R. and A.M. Grabowski, The contributions of ankle, knee and hip joint work to individual leg work change during uphill and downhill walking over a range of speeds. *Royal Society Open Science*, 2018. 5(8).